Hindawi Publishing Corporation
Advances in Condensed Matter Physics
Volume 2016, Article ID 9734610, 7 pages
http://dx.doi.org/10.1155/2016/9734610

Research Article

Ultrasensitive Anomalous Hall Effect in Ta/CoFe/Oxide/Ta Multilayers

Guang Yang, Yongye Li, Xi Chen, Jingyan Zhang, and Guanghua Yu

Department of Materials Physics and Chemistry, University of Science and Technology Beijing, Beijing 100083, China

Correspondence should be addressed to Guanghua Yu; ghyu@mater.ustb.edu.cn

Received 6 October 2016; Accepted 22 November 2016

Academic Editor: Hao Zeng

Ultrahigh anomalous Hall sensitivity has been demonstrated in Ta/CoFe/Oxide/Ta multilayers. By changing oxides (MgO and HfO_2) and annealing temperature, different annealing dependence of sensitivity was found in MgO-sample and HfO_2-sample. For the MgO-sample, the anomalous Hall sensitivity reaches 18792 Ω/T in the as-deposited state and significantly reduces as annealing temperature increases. On the contrary, the sensitivity of the as-deposited HfO_2-sample is only 765 Ω/T, while it remarkably increases with annealing temperature increasing, finally reaching 14741 Ω/T at 240°C. The opposite variation of anomalous sensitivity in two samples originates from the different change of magnetic anisotropy and anomalous Hall resistance during the annealing process. Our study provides a new perspective that both the choice of oxide material and the optimization of annealing treatment are important to the anomalous Hall sensitivity.

1. Introduction

Magnetic sensors are playing an increasing important role in daily life and industrial production, with their wide applications ranging from read heads in the hard disk [1], to the speed and rotation angle detectors in the automotive industry [2], and even to the detection of DNA and proteins [3]. The current design of magnetic sensors is based on the Hall effect in semiconductor materials or magnetoresistive effect including anisotropy magnetoresistance (AMR), giant magnetoresistance (GMR), and tunneling magnetoresistance (TMR) in magnetic materials. However, the sensors based on Hall effect and AMR effect always suffer a lower sensitivity. On the other hand, although high sensitivity can be obtained in GMR- and TMR-based sensors, the complex fabrication process with higher costs is also an obstacle. Recently, the anomalous Hall effect (AHE) of ferromagnets has attracted enormous attention owning to the abundant physics [4, 5] and potential applications [6, 7]. In 2007, Zhu and Cai [8] first demonstrated an anomalous Hall sensitivity as high as 1200 Ω/T in $[CoFe/Pt]_n$ multilayers, which is better than the conventional semiconductor Hall sensitivity (about 1000 Ω/T). Subsequently, the strategy adapted to achieve a higher sensitivity was by using ultrathin ferromagnetic films/multilayers with enhanced spin-orbit scattering and tailored magnetic anisotropy that enables large anomalous Hall resistance and low saturation field [9–13]. In particular, Lu et al. [11] obtained a sensitivity of 12000 Ω/T in $SiO_2/FePt/SiO_2$ sandwich structure films with optimized FePt composition and thickness. Zhu et al. [12] demonstrated a sensitivity of 23760 Ω/T in MgO/CoFeB/Ta/MgO multilayers by tuning the thickness of CoFeB and adjacent Ta layer. More excitingly, a very recent study has reported the anomalous Hall sensitivity up to 10^6 Ω/T, which is two orders higher than the best of semiconductors [13].

Although the achieved ultrahigh sensitivity is remarkable, the compatibility between AHE materials and CMOS technology still needs further consideration. For example, heavy metals such as Pt are always used in AHE materials to enhance the spin-orbit scattering for a large anomalous Hall resistance, while it will cause a terrible shunting effect as well as increased costs. The CoFeB/MgO heterostructure seems a more promising material system, while the commonly used oxides in CMOS technology are high-k materials such as SiO_2 and HfO_2. From the application point of view, it is better to introduce the same high-k oxides into the AHE materials. Last but not least, AHE materials generally need

additional annealing to exhibit a high sensitivity. Considering the postannealing is also essential to CMOS technology, it is necessary to further optimize the annealing process.

In this work, we demonstrate the ultrasensitive AHE in Ta/CoFe/Oxide/Ta multilayers. By changing oxides (MgO and HfO_2) and annealing temperature (T_a), opposite T_a dependence of sensitivity was found in MgO-sample and HfO_2-sample. For the MgO-sample, the anomalous Hall sensitivity reaches 18792 Ω/T in the as-deposited state and significantly reduces as T_a increases. On the contrary, the sensitivity of the as-deposited HfO_2-sample is only 765 Ω/T, while it remarkably increases with T_a increasing, finally reaching 14741 Ω/T at 240°C. Based on the angular dependent ferromagnetic resonance (FMR) measurements and temperature dependent transport measurements, the different change of sensitivity in two samples comes from the different temperature dependence of the anomalous Hall resistance and the magnetic anisotropy. This study gives new insights that the choice of oxides and the optimization of T_a are both important to obtain an ultrahigh anomalous Hall sensitivity.

2. Experiments

All samples were deposited on Si substrates by magnetron sputtering at room temperature. The sample structure is Ta(0.8)/$Co_{20}Fe_{80}$(0.8)/Oxide(0.8)/Ta(1.0) (all in nm), where the oxide is MgO or HfO_2. Thermal annealing was carried out in a vacuum furnace (better than 3×10^{-7} Torr) for 15 min without external magnetic fields. Hall bars were patterned by optical lithography combined with Ar^+ milling for transport measurements in a physical property measurement system. FMR measurements were performed in an electron spin resonance spectrometer (JEOL ESR FA-200) at X-band (9.0 GHz).

3. Results and Discussions

The anomalous Hall sensitivity is defined as $S = dR_{xy}/dH \approx R_{AH}/H_s$ [12, 14], where H_s is the perpendicular saturation field and R_{AH} is the saturated anomalous Hall resistance that can be obtained via a linear extrapolation of R_{xy} at high field to zero field. The inset of Figure 1 exhibits the anomalous Hall loops of sample Ta(0.8)/$Co_{20}Fe_{80}$(0.8)/MgO(0.8)/Ta(1.0) (in nm) in the as-deposited and different annealed states, from which the corresponding value of S is calculated. As a result, Figure 1 shows the sensitivity S as a function of the annealing temperature T_a. When T_a is 25°C (as-deposited state), S of MgO-sample has reached 18792 Ω/T. Nevertheless, the value of S decreases significantly with the increase of T_a. When T_a reaches 140°C, the value of S is 8145 Ω/T, decreasing 57% with respect to that in the as-deposited state. As T_a further increases to 240°C, the value of S is only 2572 Ω/T.

In contrast, Figure 2 shows S as a function of T_a for sample Ta(0.8)/$Co_{20}Fe_{80}$(0.8)/HfO_2(0.8)/Ta(1.0) (in nm). Different from the MgO-sample, the value of S in the as-deposited HfO_2 sample is only 765 Ω/T. When T_a increases to 180°C, the value of S appears almost unchanged. However, as T_a is above 200°C, the value of S increases dramatically. When T_a reaches 240°C, the value of S is 14741 Ω/T, which is about 19 times larger than that in the as-deposited state. It is interesting to find that the variation trend of S with respect to T_a is opposite in the MgO-sample and HfO_2-sample. To further illustrate the difference, four typical samples were chosen as below: as-deposited MgO-sample, 240°C annealed MgO-sample, as-deposited HfO_2-sample, and 240°C annealed HfO_2-sample.

As shown in Figure 3, the detailed R_{xy}-H curves of the above four samples are presented. In Figure 3(a), the curve of the as-deposited MgO-sample (black one) shows an obvious linear response without magnetic hysteresis. The saturated

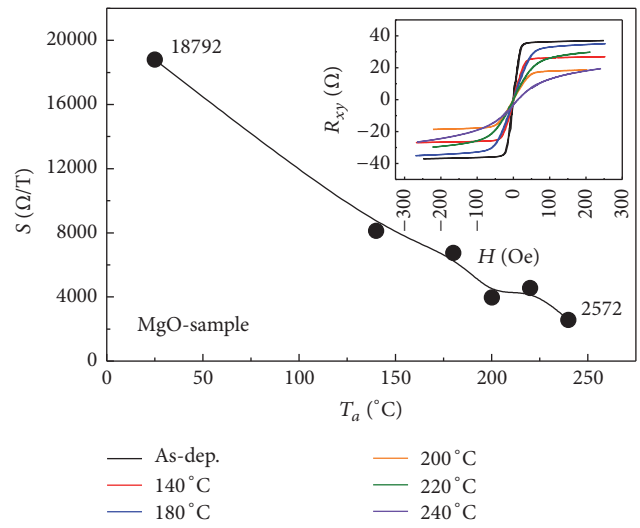

FIGURE 1: Annealing temperature dependence of the anomalous Hall sensitivity for the sample Ta(0.8)/$Co_{20}Fe_{80}$(0.8)/MgO(0.8)/Ta(1.0) (in nm). Inset: anomalous Hall loops of the sample in the as-deposited and different annealed states.

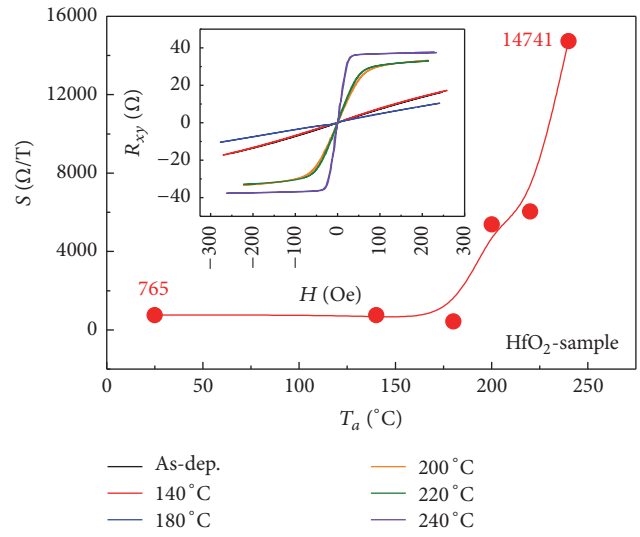

FIGURE 2: Annealing temperature dependence of the anomalous Hall sensitivity for the sample Ta(0.8)/$Co_{20}Fe_{80}$(0.8)/HfO_2(0.8)/Ta(1.0) (in nm). Inset: anomalous Hall loops of the sample in the as-deposited and different annealed states.

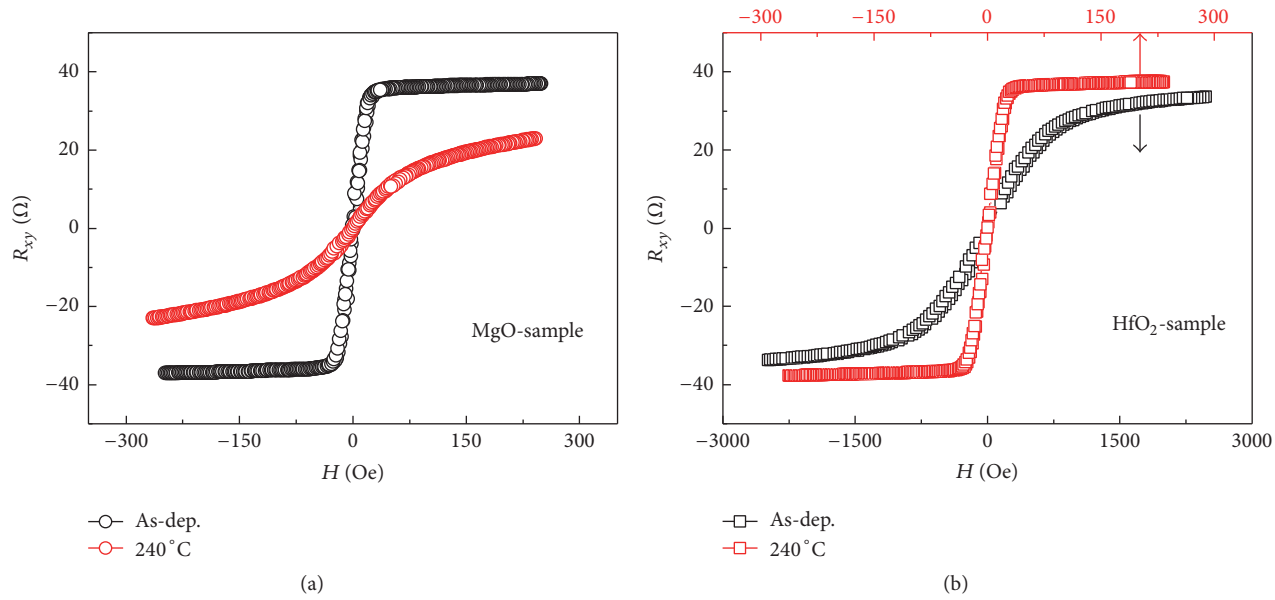

FIGURE 3: (a) R_{xy}-H curves for sample Ta(0.8)/$Co_{20}Fe_{80}$(0.8)/MgO(0.8)/Ta(1.0) (in nm) in the as-deposited and 240°C annealed states. (b) R_{xy}-H curves for sample Ta(0.8)/$Co_{20}Fe_{80}$(0.8)/HfO_2(0.8)/Ta(1.0) (in nm) in the as-deposited and 240°C annealed states.

anomalous Hall resistance R_{AH} is 35.8 Ω and the perpendicular saturation field H_s is 20 Oe. By annealing at 240°C, the linear shape of the curve began to degrade, with R_{AH} decreasing to 14.2 Ω and H_s increasing to 150 Oe. Both the reduced R_{AH} and the increased H_s are detrimental to the sensitivity, leading to a significant decrease of S from 18792 Ω/T to 2572 Ω/T. Figure 3(b) shows the R_{xy}-H curves of the as-deposited and 240°C annealed HfO_2-samples. The values of R_{AH} and H_s for the as-deposited sample are 28.5 Ω and 1000 Oe. By annealing at 240°C, the value of R_{AH} reaches 36.4 Ω while the value of H_s decreases to 30 Oe. Both the increased R_{AH} and the reduced H_s are beneficial to an ultrahigh sensitivity, leading to a significant increase of S from 765 Ω/T to 14741 Ω/T.

It is well known that the perpendicular saturation field is related to the magnetic anisotropy of the films. During the annealing process, the volume anisotropy as well as the interfacial anisotropy is likely to change [15, 16]. In order to characterize the evolution of magnetic anisotropy in the MgO- and HfO_2-samples, out-of-plane angular dependent FMR measurements were performed. The typical FMR differential absorption spectrum is shown in the inset of Figure 4(a), where the resonance field H_{res} and peak-to-peak linewidth ΔH_{pp} are defined. Figure 4(a) presents the out-of-plane angular dependent H_{res} for the as-deposited MgO-sample. Here, the angle θ_H is defined as the direction of applied magnetic field with respect to the film normal. The value of H_{res} can be fitted by Kittel's formula:

$$f = \frac{\gamma}{2\pi}\sqrt{f_1 f_2} = \frac{\gamma}{2\pi}\sqrt{H_{res}\cos(\theta_H-\theta) + H_1\cos^2\theta - H_2\cos^4\theta}\sqrt{H_{res}\cos(\theta_H-\theta) + H_1\cos 2\theta + H_2\left(3\cos^2\theta\sin^2\theta - \cos^4\theta\right)}, \quad (1)$$

where $H_1 = 2K_1/M_s + 4K_2/M_s - 4\pi M_s$ and $H_2 = 4K_2/M_s$. K_1, K_2, M_s, and θ are the first-order, second-order uniaxial anisotropy constant, the saturation magnetization, and the equilibrium angle of the magnetization vector with respect to film normal, respectively. $f = 9.0$ GHz is the frequency of AC magnetic fields in the machine. γ is the gyromagnetic ratio given as $\gamma = g\mu_B/\hbar$, where g, μ_B, and $\hbar$ are Landé factor, Bohr magneton, and Planck's constant, respectively. As shown in Figure 4(a), the experimental value of H_{res} as a function of θ_H can be well fitted, where above parameters can be obtained. Consequently, the fitting parameters g, M_s, K_1, K_2, the effective magnetic anisotropy constant $K_{eff} = K_1 - 2\pi M_s^2$, and the effective anisotropy filed $H_{eff} = 2K_{eff}/M_s$ calculated from Figures 4(a)–4(d) are listed in Table 1.

From Table 1, it is clearly seen that the variation trend of magnetic anisotropy is different in the MgO-sample and HfO_2-sample. For the as-deposited MgO-sample, both values of the effective magnetic anisotropy constant K_{eff} and the second-order uniaxial anisotropy constant K_2 are positive, indicating the sample has perpendicular magnetic anisotropy

Table 1: Fitting parameters deduced from (1) in the four samples.

	g	M_s ($\times 10^3$ emu/cm^3)	K_1 ($\times 10^6$ erg/cm^3)	K_2 ($\times 10^4$ erg/cm^3)	K_{eff} ($\times 10^5$ erg/cm^3)	H_{eff} (Oe)
MgO as-dep.	2.01	1.13	8.02	8.89	0.53	94.02
MgO 240°C	1.99	1.14	7.76	10.15	−4.09	−716.92
HfO_2 as-dep.	2.04	1.14	7.71	2.47	−5.4	−942.60
HfO_2 240°C	2.04	1.12	8.10	1.01	2.07	369.26

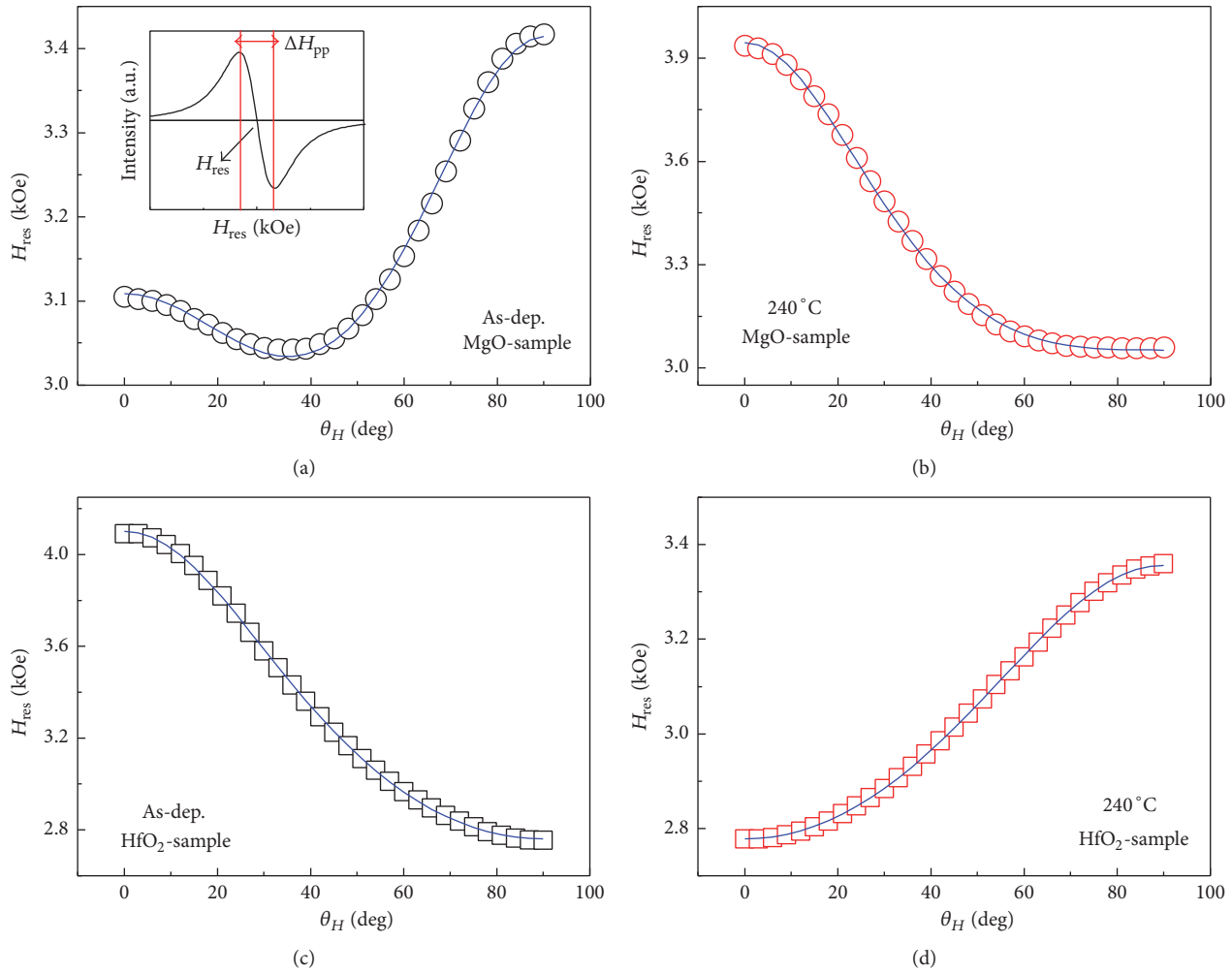

Figure 4: (a)-(b) Out-of-plane angular dependent resonance fields H_{res} for sample Ta(0.8)/$Co_{20}Fe_{80}$(0.8)/MgO(0.8)/Ta(1.0) (in nm) in the as-deposited and 240°C annealed states. Hollow circles and solid lines represent experimental data and theoretical fitting of H_{res}. Inset: typical FMR differential absorption spectra where the resonance field H_{res} and peal-to-peak linewidth ΔH_{pp} are defined. (c)-(d) Out-of-plane angular dependent resonance fields H_{res} for sample Ta(0.8)/$Co_{20}Fe_{80}$(0.8)/HfO_2(0.8)/Ta(1.0) (in nm) in the as-deposited and 240°C annealed states. Hollow diamonds and solid lines represent experimental data and theoretical fitting of H_{res}.

(PMA) [17]. For the sample with PMA, the perpendicular direction is the easy magnetization axis; thus the perpendicular saturation filed H_s is small. It is also important to point out that since the calculated effective anisotropy field H_{eff} is very small (only about 94 Oe), the R_{xy}-H curve will not exhibit the obvious coercivity. For the 240°C annealed MgO-sample, the calculated values of K_{eff} and K_2 are -4.09×10^5 erg/cm^3 and 1.02×10^5 erg/cm^3, respectively. Considering the value of K_{eff} is negative and $K_2 < -(1/2)K_{\text{eff}}$, the annealed MgO-sample has in-plane magnetic anisotropy (IMA) [17]. For the sample with IMA, the perpendicular direction is the difficult magnetization axis; thus the value of H_s will be very large. On the other hand, for the as-deposited HfO_2-sample, the value of K_{eff} is negative and $K_2 < -(1/2)K_{\text{eff}}$, representing a typical IMA character. However, by annealing at 240°C, both the values of K_{eff} and K_2 change to positive, indicating the 240°C annealed HfO_2 sample has PMA with a small H_s. Therefore, the variation trend of magnetic anisotropy

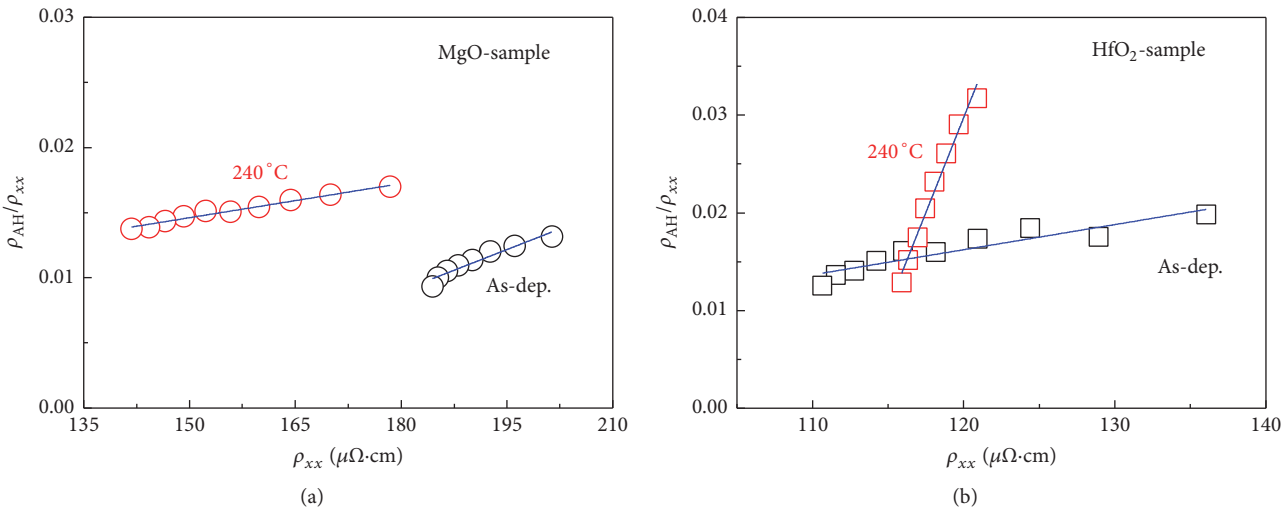

FIGURE 5: (a) ρ_{AH}/ρ_{xx} versus ρ_{xx} for sample Ta(0.8)/$Co_{20}Fe_{80}$(0.8)/MgO(0.8)/Ta(1.0) (in nm) in the as-deposited and 240°C annealed states. (b) ρ_{AH}/ρ_{xx} versus ρ_{xx} for sample Ta(0.8)/$Co_{20}Fe_{80}$(0.8)/HfO_2(0.8)/Ta(1.0) (in nm) in the as-deposited and 240°C annealed states.

during annealing is opposite in the MgO-sample and HfO_2-sample. For MgO-sample, the magnetic anisotropy changes from PMA to IMA, resulting in a significant increase of H_s, while, for HfO_2-sample, the magnetic anisotropy changes from IMA to PMA, leading to a remarkable decrease of H_s.

For the ferromagnetic metal (FM)/Oxide heterostructures, the interfacial magnetic anisotropy plays a dominated role [16]. In theory, first-principles calculation has been used to study the FM/Oxide interface, showing that the interfacial magnetic anisotropy is strongly affected by the hybridization between FM-3*d* and O-2*p* orbits [18, 19]. In addition, previous researches have reported that the orbital hybridization between FM and oxide is sensitive to the annealing process [20, 21]. By annealing, the activated oxygen atoms could migrate to the interface, producing a bonding between FM atoms and oxygen atoms. It is necessary to point out that the degree of bonding is important to the orbital hybridization, where an optimized bonding is beneficial to PMA, whereas the excessive and insufficient bonding will lead to a degradation of PMA [22]. Here in our samples, the enthalpy of formation (ΔH_f) for MgO is −601.6 kJ/mol, larger than that for HfO_2 (−1144.7 kJ/mol). It means that the combination between Hf and O is more stable than that between Mg and O. Therefore, during the deposition and annealing process, MgO is more likely to deviate the stoichiometric ratio and transfer oxygen atoms to the adjacent CoFe layer, leading to the final difference of the FM-O bonding degree for the two samples. According to our recent work, the oxygen migration direction during annealing process may be inverse at different FM/Oxide interfaces [23]. However, since the oxygen migration could also be affected by the film thickness and annealing temperature and so forth, the specific differences about oxygen migration in the two samples need further investigation.

In addition to H_s, AHE sensitivity is also related to R_{AH}, whose value represents the magnitude of AHE. Previous work has reported that the annealing process will affect the intrinsic or extrinsic mechanisms, leading to a variation of AHE [24, 25]. To explain the change of R_{AH} in the MgO- and HfO_2-sample as shown in Figure 3, contributions to the AHE by different mechanisms were analyzed. In general, $\rho_{AH} = a\rho_{xx} + b\rho_{xx}^2$, where ρ_{AH} is the saturated anomalous Hall resistivity, ρ_{xx} is the longitudinal resistivity, a represents the skew scattering contribution, and b represents the side jump as well as the intrinsic contribution [26–30]. It is necessary to point out that the thickness change during annealing is eliminated; thus ρ_{AH} is equivalent to R_{AH}. The coefficients a and b can be obtained by plotting ρ_{AH}/ρ_{xx} as a function of ρ_{xx} and linear fitting to the experimental data. Figure 5(a) shows the linear fitting for MgO-sample in the as-deposited and 240°C annealed states. The values of a and b are −0.029 and 2.12×10^{-4} $\mu\Omega^{-1}$ cm^{-1} in the as-deposited state, respectively. By annealing at 240°C, the values of a and b change to 0.002 and 8.74×10^{-5} $\mu\Omega^{-1}$ cm^{-1}, respectively. Although the sign of a alters from negative to positive, both the values of $|a|$ and $|b|$ decrease by one order of magnitude, finally weakening the AHE. For the HfO_2-sample, the values of a and b are −0.015 and 2.57×10^{-4} $\mu\Omega^{-1}$ cm^{-1} in the as-deposited state, respectively. By annealing at 240°C, both the values of $|a|$ and $|b|$ increase by one order of magnitude, reaching −0.437 and 3.89×10^{-3} $\mu\Omega^{-1}$ cm^{-1}, respectively. The competitive relation between a and b will affect not only the value but also the sign of ρ_{AH}. Considering the large enhancement of $|b|$ as well as the same positive sign between b and ρ_{AH}, it suggests that the influence of b on AHE is improved during annealing process for the HfO_2-sample. Above analysis gives strong evidence that the variation trend of AHE is different during the annealing process in the MgO- and HfO_2-sample. For the MgO-sample, both the intrinsic and extrinsic contributions to AHE are weakened by annealing, resulting in the significant decrease of R_{AH} as shown in Figure 3(a). In contrast, the side jump and the intrinsic contributions are remarkably enhanced, leading to the final increase of R_{AH} as shown in Figure 3(b).

4. Conclusions

In conclusion, the ultrasensitive AHE was demonstrated in Ta/CoFe/Oxide/Ta multilayers. For sample Ta/CoFe/MgO/Ta, AHE sensitivity is as high as 18792 Ω/T in the as-deposited state, while the value decreases significantly as the annealing temperature increases. For sample Ta/CoFe/HfO_2/Ta, the value of sensitivity is small in the as-deposited state but increases to 14741 Ω/T by 240°C annealing. The opposite variation of AHE sensitivity in two samples originates from the different change of magnetic anisotropy and anomalous Hall resistance during the annealing process. This work gives new insights that both the choice of oxide material and the optimization of annealing treatment play an important role in the anomalous Hall sensitivity.

Competing Interests

The authors declare that there is no conflict of interests regarding the publication of this paper.

Acknowledgments

This work was supported by the National Basic Research Program of China (2015CB921502) and the Natural Science Foundation of China (51331002, 51371027, and 11504019).

References

[1] J. M. Daughton, "GMR and SDT sensor applications," *IEEE Transactions on Magnetics*, vol. 36, no. 5, pp. 2773–2778, 2000.

[2] C. P. O. Treutler, "Magnetic sensors for automotive applications," *Sensors and Actuators, A: Physical*, vol. 91, no. 1-2, pp. 2–6, 2001.

[3] S. G. Grancharov, H. Zeng, S. Sun et al., "Bio-functionalization of monodisperse magnetic nanoparticles and their use as biomolecular labels in a magnetic tunnel junction based sensor," *The Journal of Physical Chemistry B*, vol. 109, no. 26, pp. 13030–13035, 2005.

[4] N. Nagaosa, J. Sinova, S. Onoda, A. H. MacDonald, and N. P. Ong, "Anomalous Hall effect," *Reviews of Modern Physics*, vol. 82, no. 2, pp. 1539–1592, 2010.

[5] Y. Tian, L. Ye, and X. Jin, "Proper scaling of the anomalous hall effect," *Physical Review Letters*, vol. 103, no. 8, Article ID 087206, 2009.

[6] J. Moritz, B. Rodmacq, S. Auffret, and B. Dieny, "Extraordinary Hall effect in thin magnetic films and its potential for sensors, memories and magnetic logic applications," *Journal of Physics D: Applied Physics*, vol. 41, no. 13, Article ID 135001, 2008.

[7] A. Gerber, "Towards Hall effect spintronics," *Journal of Magnetism and Magnetic Materials*, vol. 310, no. 2, pp. 2749–2751, 2007.

[8] Y. Zhu and J. W. Cai, "Ultrahigh sensitivity Hall effect in magnetic multilayers," *Applied Physics Letters*, vol. 90, no. 1, Article ID 012104, 2007.

[9] S. L. Zhang, J. Teng, J. Y. Zhang et al., "Large enhancement of the anomalous Hall effect in Co/Pt multilayers sandwiched by MgO layers," *Applied Physics Letters*, vol. 97, no. 22, Article ID 222504, 2010.

[10] J. Zhang, G. Yang, S. Wang et al., "Ultrahigh anomalous hall sensitivity in Co/Pt multilayers by interfacial modification," *Applied Physics Express*, vol. 6, no. 10, Article ID 103007, 2013.

[11] Y. M. Lu, J. W. Cai, H. Y. Pan, and L. Sun, "Ultrasensitive anomalous Hall effect in SiO_2/Fe-Pt/SiO_2 sandwich structure films," *Applied Physics Letters*, vol. 100, no. 2, Article ID 022404, 2012.

[12] T. Zhu, P. Chen, Q. H. Zhang, R. C. Yu, and B. G. Liu, "Giant linear anomalous Hall effect in the perpendicular CoFeB thin films," *Applied Physics Letters*, vol. 104, no. 20, Article ID 202404, 2014.

[13] G. Kopnov and A. Gerber, "MegaOhm extraordinary Hall effect in oxidized CoFeB," *Applied Physics Letters*, vol. 109, no. 2, Article ID 022404, 2016.

[14] G. X. Miao and G. Xiao, "Giant Hall resistance in Pt-based ferromagnetic alloys," *Applied Physics Letters*, vol. 85, no. 1, pp. 73–75, 2004.

[15] T. Maeda, T. Kai, A. Kikitsu, T. Nagase, and J.-I. Akiyama, "Reduction of ordering temperature of an FePt-ordered alloy by addition of Cu," *Applied Physics Letters*, vol. 80, no. 12, pp. 2147–2149, 2002.

[16] S. Ikeda, K. Miura, H. Yamamoto et al., "A perpendicular-anisotropy CoFeB–MgO magnetic tunnel junction," *Nature Materials*, vol. 9, no. 9, pp. 721–724, 2010.

[17] E. Y. Vedmedenko, H. P. Oepen, and J. Kirschner, "Microstructure of the spin reorientation transition in second-order approximation of magnetic anisotropy," *Physical Review B*, vol. 66, no. 21, Article ID 214401, 2002.

[18] H. X. Yang, M. Chshiev, B. Dieny, J. H. Lee, A. Manchon, and K. H. Shin, "First-principles investigation of the very large perpendicular magnetic anisotropy at Fe—MgO and Co—MgO interfaces," *Physical Review B*, vol. 84, no. 5, Article ID 054401, 2011.

[19] K. H. Khoo, G. Wu, M. H. Jhon et al., "First-principles study of perpendicular magnetic anisotropy in CoFe/MgO and CoFe/$Mg_3B_2O_6$ interfaces," *Physical Review B*, vol. 87, no. 17, Article ID 174403, 2013.

[20] X. Chen, C. Feng, Z. Long Wu et al., "Interfacial oxygen migration and its effect on the magnetic anisotropy in Pt/Co/MgO/Pt films," *Applied Physics Letters*, vol. 104, no. 5, Article ID 052413, 2014.

[21] G. Yang, J.-Y. Zhang, S.-G. Wang et al., "Magnetization reorientation induced by interfacial structures in ultrathin disordered FePt film sandwiched by SiO_2 layers," *Applied Surface Science*, vol. 353, pp. 489–493, 2015.

[22] A. Manchon, C. Ducruet, L. Lombard et al., "Analysis of oxygen induced anisotropy crossover in Pt/Co/MOx trilayers," *Journal of Applied Physics*, vol. 104, no. 4, Article ID 043914, 2008.

[23] G. Yang, J.-Y. Zhang, S.-L. Jiang et al., "Effect of oxygen migration on magnetic anisotropy and damping constant in perpendicular Ta/CoFeB/Gd/MgO/Ta multilayers," *Applied Surface Science*, 2016.

[24] S.-L. Jiang, X. Chen, X.-J. Li et al., "Anomalous Hall effect engineering via interface modification in Co/Pt multilayers," *Applied Physics Letters*, vol. 107, no. 11, Article ID 112404, 2015.

[25] S.-L. Jiang, G. Yang, J. Teng, Q.-X. Guo, L.-L. Li, and G.-H. Yu, "Interface-engineered spin-dependent transport in perpendicular Co/Pt multilayers," *Applied Surface Science*, vol. 387, pp. 375–378, 2016.

[26] M.-C. Chang and Q. Niu, "Berry phase, hyperorbits, and the Hofstadter spectrum: semiclassical dynamics in magnetic Bloch bands," *Physical Review B - Condensed Matter and Materials Physics*, vol. 53, no. 11, pp. 7010–7023, 1996.

[27] D. Hou, Y. Li, D. Wei, D. Tian, L. Wu, and X. Jin, "The anomalous Hall effect in epitaxial face-centered-cubic cobalt films," *Journal of Physics Condensed Matter*, vol. 24, no. 48, Article ID 482001, 2012.

[28] J. Smit, "The spontaneous hall effect in ferromagnetics II," *Physica*, vol. 24, no. 1–5, pp. 39–51, 1958.

[29] L. Berger, "Side-jump mechanism for the hall effect of ferromagnets," *Physical Review B*, vol. 2, no. 11, pp. 4559–4566, 1970.

[30] A. Crépieux and P. Bruno, "Theory of the anomalous hall effect from the Kubo formula and the Dirac equation," *Physical Review B*, vol. 64, no. 1, Article ID 014416, 2001.